Construction and Building Materials 482 (2025) 141495

Contents lists available at ScienceDirect

Construction and Building Materials

journal homepage: www.elsevier.com/locate/conbuildmat

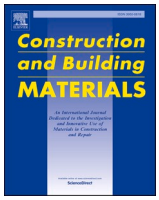

Hygrothermal performance of compressed earth blocks incorporating quackgrass straw

Gratien Kiki [a,*], Romain Rémond [b], Sahbi Ouertani [b], Aristide Houngan [c], Philippe André [a]

[a] Building Energy Monitoring and Simulation, Liege University, Avenue de Longwy 185, Arlon 6700, Belgium
[b] Université de Lorraine, INRAE, LERMAB, Épinal 88000, France
[c] Laboratoire Pluridisciplinaire de l'Enseignement Technique, Université Nationale des Sciences Technologies Ingénierie et Mathématiques, Abomey BP 133, Benin

ARTICLE INFO

Keywords:
Hygrothermal performance
CEB
Quackgrass straw
Heat and mass transfer
Simulation

ABSTRACT

Biosourced earth materials represent a sustainable alternative to conventional building materials in the effort to fight and adapt to the effects of global warming in the construction sector. These materials have hygrothermal properties that enhance the thermal insulation of buildings and facilitate passive control of the relative humidity in indoor environments. The aim of this work is to study the hygrothermal properties of compressed clay – quackgrass straw blocks stabilised with 8*wt*% cement. Thermal characterisation of this material shows that the addition of 0 to 1.5*wt*% quackgrass straw in 0.5 increments improves the thermal conductivity of the clay material by 19%, from $0.74 W.m^{-1}.K^{-1}$ to $0.6 W.m^{-1}.K^{-1}$ at 40%*RH*. The simultaneous search for good thermal and mechanical performance of the material showed that the presence of 1*wt*% quackgrass straw in the Compressed Earth Block (CEB) was a good compromise. However, despite the incorporation of a biosourced material (quackgrass straw), CEB_8-1 exhibited a moisture adsorption capacity that was not significantly affected in comparison to the earthen control material (CEB_8-0). At 85%*RH*, the Equilibrium Moisture Content (EMC) of CEB_8-1 was determined to be $2.57\% kg.kg^{-1}$, while that of CEB_8-0 was found to be $2.92\% kg.kg^{-1}$. Furthermore, implementation of these properties into numerical simulations of hygrothermal transfer through CEB_8-0 and CEB_8-1 materials gives results consistent with experimentation. This is reflected in statistical accuracy indicators (MBE and CV(RMSE)) close to 0.

1. Introduction

The efforts to fight against climate change and the depletion of natural resources depend in part on the implementation of energy-efficient, thermally comfortable buildings with low greenhouse gas (GHG) emissions. This is all the truer as the building sector plays a major role in global warming. It is responsible for 32% of gas emissions, of which about 11% are due to materials and construction, and the rest to the energy used to operate buildings, i.e. about 30% of global energy production in 2022 [1]. According to the International Energy Agency (IEA), if no action is taken to improve the energy efficiency of buildings, global energy consumption in the building sector could increase by around 50% [2].

In addition to considerations of aesthetic appeal, a building will be evaluated primarily based on the level of comfort it provides to its occupants and its energy performance. A building energy performance is indicative of the quality of its energy consumption [3]. The term can be defined by the interaction of six factors: climate, the building envelope, the building energy services, its operation, occupant behavior and the quality of the indoor environment provided [4]. In light of the aforementioned, Horne & Hayles [5] assume that the energy performance of the envelope and its durability represent the most pivotal factors in the search of optimal energy performance in buildings. Indeed, several studies estimate that over 60% of the thermal load in buildings can be attributed to heat transfer through the envelope [6–8]. Limiting this heat transfer by using materials with better thermal properties would reduce the energy consumed by HVAC (Heating Ventilation and Air Conditioning) systems to ensure thermal comfort.

Considering the substantial energy demands associated with heating and cooling buildings, it is obvious that the conventional materials (such as concrete) employed in construction do not exhibit the required thermal properties to address the climate challenge confronting the

* Corresponding author.
E-mail addresses: gjd.kiki@uliege.be (G. Kiki), romain.remond@univ-lorraine.fr (R. Rémond), ouertani.sahbi@yahoo.fr (S. Ouertani), hounaris@yahoo.fr (A. Houngan), p.andre@uliege.be (P. André).

https://doi.org/10.1016/j.conbuildmat.2025.141495
Received 9 December 2024; Received in revised form 7 March 2025; Accepted 23 April 2025

planet. Earth materials present a good alternative. The minimal energy requirements for utilization and the extensive availability of these materials render them environmentally friendly and accessible to all. In their 2017 study, Niroumand et al. [9] define raw earth as a sustainable building material that considers health, thermal comfort, and economic criteria. Earth materials have intriguing hygrothermal characteristics that, when optimally harnessed, guarantee energy savings in buildings. To illustrate, Zhang et al. [10] have employed CEBs (Compressed Earth Blocks) with thermal conductivities spanning from 0.52 to $0.93 W.m^{-1}.K^{-1}$, depending on the density of the materials in question. The highest conductivity was observed in specimens with a density of $2100 kg.m^{-3}$. In comparison, concrete blocks with a similar density ($2000 kg.m^{-3}$), which are commonly used in building walls, exhibited a conductivity of $1.7 W.m^{-1}.K^{-1}$ [11]. Table 1 provides a concise synopsis of the thermal properties of selected earth materials as documented in the existant literature. The thermal conductivities of these materials have been determined as a function of their relative humidity or water content, but also as a function of the content of incorporated biosourced fibres. In most cases, these bio-based materials improve the thermal properties of earth matrices. For instance, [12] observed a 75 %, 65 %, and 54 % reduction in thermal conductivity when 6 wt% of barley straw, hemp shiv, and corn cob, respectively, were incorporated into the soil matrix (Table 1).

Earth materials also have the ability to passively control humidity in indoor environments [21] as they are hygroscopic. However, most of the research conducted on these materials has primarily focused on their mechanical and thermal properties, with relatively little attention paid to their hygric properties. This trend was corroborated by the findings of Turco et al. [22]. After a comprehensive review of 86 articles on earth construction materials from around the world, the authors concluded that 89% of them focused on determining their mechanical properties, while only 33.3% addressed their thermal properties. None of the studies considered the hygroscopic properties of these materials. Furthermore, this study identified a number of studies that emphasised the hygroscopic nature of earth materials by determining their Equilibrium Moisture Content (*EMC*) and their vapor diffusion resistance factor (μ) (Table 1). Despite the endeavours of the scientific community to accelerate progress in this domain, Benin is falling behind in taking account the hygroscopic characteristics of these materials. For instance, of the approximately fifteen articles on earth construction materials in Benin identified in this study (Table 2), only one addressed the hygroscopic properties of these materials. This was the study carried out by Houngan et al. [23] (Table 2). However, a large part of the country, particularly in the southern region, is subject to a humid tropical climate (70 to 95%*RH*), which has a considerable impact on the actual performance of these materials.

It is a widely acknowledged fact that humidity is a primary factor to

Table 1
Hygrothermal properties of a number of earthen materials in the world.

Constructive technique	Materials	Density 'ρ' ($kg.m^{-3}$)	Thermal conductivity 'λ' ($W.m^{-1}.K^{-1}$)	EMC (%.$kg.kg^{-1}$)	Vapor diffusion resistance factor 'μ' (–)	Ref
CEB	Earth	1500 – 2100	0.52 – 0.93	4.5 – 4.2 at 98%*RH*	–	[10]
	Earth + barley straw [0 – 6*wt*%]	1891 ± 54 – 1100 ± 49	0.57 ± 0.03 – 0.14 ± 0.01	2.7 – 3.3 at 94%*RH*	4.9 ± 0.3 – 7 ± 0.3 (wet cup)	[12]
	Earth + hemp shiv [0 – 6*wt*%]	1891 ± 54 – 1271 ± 16	0.57 ± 0.03 – 0.20 ± 0.01	2.7 – 3.4 at 94%*RH*	4.9 ± 0.3 – 6.1 ± 0.2 (wet cup)	
	Earth + corn cob [0 – 6*wt*%]	1891 ± 54 – 1565 ± 18	0.57 ± 0.03 – 0.26 ± 0.01	2.7 – 3.8 at 94%*RH*	4.9 ± 0.3 – 5.1 ± 0.7 (wet cup)	
Extruted earth bricks	Earth brick 1	2060	0.59	6 at 95%*RH*	7 (dry cup) / 3 (wet cup)	[13]
	Earth brick 2	2030	0.56	5.2 at 95%*RH*	9 (dry cup) / 6 (wet cup)	
	Earth brick 3	2020	0.52	5.3 at 95%*RH*	19 (dry cup)/ 5 (wet cup)	
	Earth brick 4	1940	0.56	4.4 at 95%*RH*	7 (dry cup) / 4 (wet cup)	
	Earth brick 5	2070	0.47	4.4 at 95%*RH*	14 (dry cup)/ 7 (wet cup)	
	Earth brick 1 + lime [0 – 5*wt*%]	1989 – 1829	1.02 – 1.18 at 0 – 85%*RH* (0*wt*% of lime) 0.74 – 0.79 at 0 – 85%*RH* (5*wt*% of lime)	3.5 – 5.1 at 96%*RH*	9.1 – 8.1 (wet cup)	[14]
	Earth brick 2 + lime [0 – 5*wt*%]	2046 – 1863	0.97 – 1.26 at 0 – 85%*RH* (0*wt*% of lime) 0.81 – 1.06 at 0 – 85%*RH* (5*wt*% of lime)	3.7 – 4.8 at 96%*RH*	11.1 – 9.4 (wet cup)	
	Earth brick 3 + lime [0 – 5*wt*%]	1992 – 1843	1.20 – 1.23 at 0 – 85%*RH* (0*wt*% of lime) 0.88 – 0.95 at 0 – 85 % RH (5 wt % of lime)	4.9 – 7.2 at 96%*RH*	8.8 – 9.3 (wet cup)	
Adobe	Earth	1762 – 1798 at 0 – 96%*RH*	0.77 – 0.95 at 0 – 96%*RH*	5.2 at 96%*RH*	–	[15]
	Earth	2024	0.85 – 1.05 at 40 – 95%*RH*	3.6 at 95%*RH*	–	[16]
	Earth	1988	0.85 – 1.03 at 40 – 95%*RH*	3.3 at 95%*RH*	–	
	Earth	1672	0.85 – 1.01 at 40 – 95%*RH*	2.2 at 95%*RH*	–	
Rammed earth	Earth	–	0.63 – 1.20 at 0 – 14*wt*% of water content	4.2 at 98%*RH*	–	[17]
	Earth + sand = Mix	2084	1.43 – 1.54 at 0 – 14.5*wt*% of water content	1.6 at 98%*RH*	14 (wet cup)	[18]
	Mix + 1*wt*% of lignin sulfonate	2086	1.87 – 1.91 at 0 – 15.6% of water content	1.8 at 98%*RH*	16.8 (wet cup)	
	Mix + 1*wt*% of tannin	2057	1.43 – 1.46 at 0 – 16% of water content	1.7 at 98%*RH*	11.2 (wet cup)	
	Mix + 0.25*wt*% of wool	2069	1.44 – 1.58 at 0 – 15.8% of water content	1.7 at 98%*RH*	14,1 (wet cup)	
Cob	Earth + 2.5*wt*% flax straw	1650	0.48 –1.31 at 1 – 21% water content	2 at 90%*RH*	12.9 (dry cup)	[19]
	Earth + 3*wt*% straw fibers	1654	0.167 – 0.197 at 10 – 40°*C*	3.7 at 90%*RH*	18.5 (dry cup)	[20]

Table 2
Characteristics of earthen materials produced in Benin.

Year	Material	Properties studied					Ref
		Physical	Mechanical	Thermal	Mass transfer	Durability	
2011	Cement – stabilised laterite		–	–	$EMC = 10.2$	–	[23]
	cement – wood composite	–	–	–	$EMC = 4.8$	–	
2015	Composite of clay, rice stalks and cowpea infusion (banco granary)	$\rho = 1565$	$DCS = [3.14; 4.95]$ $\sigma = [2.1; 2.3]$	$\lambda = [0.87; 1]$ $E = [1290; 1428]$ $a = [4.54; 4.98]$	–	–	[24]
2015	CEB stabilised with 10 %wt cement and containing cotton waste $[0; 50\%vt]$	$\rho = 1565$	$DCS = [1.5; 3.2]$ $\sigma = [0.24; 0.75]$	–	–	$Cb = [7; 32]$ $Ca = [0.8; 5.7]$	[25]
2016	CEB stabilised with 10 %wt cement and containing sawdust $[0; 8\%wt]$	–	$DCS = [1; 4.3]$ $\sigma = [0.23; 0.34]$	$\lambda = [0.85; 1.7]$ $E = [1318; 1811]$ $a = [4.16; 8.91]$	–	–	[26]
2017	CEB containing kenaf fibers (0 and 1.2 % wt) of size $[10; 30mm]$	$\varepsilon = [18; 21.3]$	$DCS = [4.1; 6.2]$	$\lambda = [0.95; 2.08]$	–	–	[27]
2017	CEB stabilised with 10 %wt cement and containing crushed waste glass $[0; 60\ \%wt]$	–	$DCS = [2.4; 5.3]$ $\sigma = [0.7; 2]$	–	–	–	[28]
	Fired clay brick containing crushed glass waste $[0; 60\ \%wt]$	–	$DCS = [14.6; 16.6]$ $\sigma = [3.6; 8]$	–	–	–	
2018	Fired clay brick containing expanded polystyrene $[0; 100\ \%vt]$	$\rho = [1199; 1750]$	$DCS = [3.08; 9.51]$ $\sigma = [0.32; 1.22]$	–	–	–	[29]
2018	Fired compressed clay containing coal ash $[0; 20\%wt]$	–	$DCS = [6.6; 9.2]$ $\sigma = [1.3; 3.9]$	$\lambda = [0.58; 0.68]$	–	–	[30]
2019	CEB containing kenaf fibers $[0.5; 1.5\%wt]$	$\rho = 2138$ $\varepsilon = [15.5; 19]$	$DCS = [3.1; 4]$ $\sigma = [0.93; 1.4]$	$\lambda = [1.2; 1.7]$	–	–	[31]
2019	Banco: adobe reinforced with rice straw $[0; 37\%vt]$	$\rho = [1550; 1830]$	$DCS = [2.72; 4.45]$ $\sigma = [0.3; 1.05]$	–	–	–	[32]
2020	Compacted cement mortar concrete containing laterite $[0; 30\%wt]$ and waste glass $[0 - 30\%wt]$	$\rho = [2319; 2444]$	$DCS = [31; 66]$ $\sigma = [3.1; 7.9]$	–	–	$A = [3.9; 5.1]$	[33]
2021	Laterite stabilised with 26 % cement and containing millet pods $[0; 6\%wt]$	$\rho = [1650 - 2100]$ $\varepsilon = [12; 46]$	–	$\lambda = [0.61; 1.8]$ $E = [775; 2157]$ $a = [3; 6.25]$	–	–	[34]
2023	CEB stabilised with 8% cement and containing quackgrass straw $[0; 1.5\%wt]$	$\rho = [1692; 1932]$ $\varepsilon = [27; 33]$ $\Delta l_c/l = [0; 16.66]$	$DCS = [3; 5.1]$ $WCS = [0.56; 3.85]$ $S_{ef} = [1040; 2640]$	–	–	$Cb = [6.43; 22.65]$ $Ca = [7.1; 29.7]$ $Er = [6.6; 32.6]$	[35]
2023	Laterite Adobe made with water from the decoction of shea and néré nuts	$\Delta l_c/l = [3.01; 4.06\%]$	$DCS = [0.97; 2.56]$	–	–	$Cb = [3.44; 5.56]$ $A = [4.34; 8.5]$ $Er = [2.33; 12]$	[36]

ρ: density ($kg.m^{-3}$)
ε: Water accessible porosity (%)
$\Delta l_c/l$: dimensional variation ($mm.m^{-1}$)
σ: flexural strength (MPa)
DCS: Dry Compressive Strength (MPa)
WCS: Wet Compressive Strength (MPa)
S_{ef}: Structural efficiency ($J.kg^{-1}$)
λ: thermal conductivity ($W.m^{-1}.K^{-1}$)
E: Thermal Effusivity ($J.K^{-1}.m^{-2}.s^{-0.5}$)
a: thermal diffusivity ($.10^{-7}$ $m^2.s^{-1}$)
EMC: Equilibrium Moisture Content ($\%.kg.kg^{-1}$)
Cb: capillary water absorption ($g.cm^{-2}$)
Ca: abrasion resistance ($cm^2.g^{-1}$)
A: water absorption (%)
Er: erosion resistance time ($mm.h^{-1}$)

the development of 75 – 80% of building-related issues [37]. An indoor environment that is too damp may result in the formation of mould on walls, as well as discomfort for occupants, including allergies and breathing difficulties. Additionally, over-consumption of HVAC (heating, ventilation and air conditioning) systems may occur. Conversely, the hygroscopic properties of earth materials facilitate enhanced respiratory comfort, dermal humidity, superior indoor air quality and the mitigation of the deterioration of artefacts and buildings. Furthermore, they assist in reducing the energy consumption associated with the humidification or dehumidification of buildings. For instance, following a 10-month monitoring period of a stabilized rammed earth building, Allison and Hall [38] demonstrated that this material is able to markedly reduce the range of variation in the relative humidity of the ambient air. The numerical simulations conducted in this study demonstrated energy savings on the humidification and dehumidification load, with a range of 44.4 to 65.4% depending on the scenario (continuous or intermittent cooling). [39] also demonstrated, through in situ measurements, the material's capacity to attenuate fluctuations in the building's relative humidity. The authors primarily attribute this regulatory effect to the high buffering capacity of the earth envelope and its sorption capacity. Belarbi et al. [40] have demonstrated the value of considering coupled heat and moisture transfer through bio-based earthen envelopes in improving the energy efficiency of buildings. The authors observed an 11.5% reduction, with hygrothermal transfer occurring at the expense of thermal transfer. Knowing that these transfers depend mainly on the hygrothermal behaviour of these envelopes, it is therefore necessary to determine the thermal and hygroscopic properties of the materials from which they are made. This approach is essential if we are to better assess the influence of bio-based earth envelopes on the energy performance of buildings and the hygrothermal comfort of their occupants

This article is devoted to the hygrothermal characterization of a clay – quackgrass straw eco-material. To achieve this objective, the study presents the equipment, and the various methods adopted. Then, the discussion and results of the hygrothermal characterization, along with simulations of the hygrothermal behavior of the material, are presented. Finally, the main findings of the study are presented in the last section.

2. Materials and methods

2.1. Clay – quackgrass straw CEBs

Clay – quackgrass straw CEBs were obtained by mixing an earth matrix (clay + 0/5 granite dust) with 8wt% Portland cement and 0 to 1.5wt% quackgrass straw. The addition of 0/5 granite dust (around

36*wt*%) was necessary to ensure the granulometry and plasticity of the clay were in accordance with the physical characteristics of a soil matrix intended for the manufacture of CEBs, as recommended by the standard XP P 13–901 [28,41]. Cement was incorporated into the soil matrix to enhance the mechanical properties and durability of the CEBs. The incorporation of quackgrass straw is attributed to the objective of enhancing the hygrothermal properties of the material. The use of CEBs and their physical, mechanical and durability properties have been presented in [26]. From the study, only CEBs containing 0% (CEB_{8-0}), 0.5% ($CEB_{8-0.5}$) and 1% (CEB_{8-1}) quackgrass straw can be used in building envelopes due to their mechanical and durability properties. Therefore, the present study will only focus on these three formulations. Table 3 shows the composition and properties of the materials determined in [35] and required in the present study.

2.2. Thermal characterization of clay – quackgrass straw CEBs

The thermal properties of the composites were measured using the Hot Disk TPS 500S instrument based on the transient planar source method as described in ISO 22007–2. In this method, a heat flux generated by a short electrical pulse in a hot disk probe is sent through two theoretically identical specimens sandwiching the thermal probe. This probe, which acts as both a heat source and a temperature sensor, is used to record temperature changes over a relatively short period of time (a few seconds) so that the thermal conditions of the external environment do not affect the measurements (semi-infinite medium hypothesis).

For this purpose, samples of clay – quackgrass straw with dimensions of $10 \times 10 \times 2(cm^3)$ were used for thermal testing with the Hot Disk 5501 Kapton probe and a radius of 6.403*mm* (Fig. 1). The heating powers injected by the probe through the samples tested ranged from 60 to 80*mW*, with measurements lasting between 40 and 80*seconds*. The thermal diffusivity ($a = 0.68\, mm^2.s^{-1}$) of a CEB stabilised with 8*wt*% cement [42] was utilised to estimate the heat penetration depth at 7.4*mm* for a minimum edge distance of 20*mm* between the clay and quackgrass straw samples. This verifies the semi-infinite medium hypothesis.

Furthermore, given that the water content is the factor that most influences the thermal properties of earth materials, the thermal conductivities were measured on samples initially equilibrated in a climatic chamber at 35°*C* and 0%*RH*, 40%*RH* and 85%*RH*. At each of these exposure levels, three pairs of samples per CEB formulation were used, with measurements repeated three times on each pair. In total, 12 pairs of quackgrass straw clay samples were used for a series of 36 thermal measurements for the CEB_{8-0}, the $CEB_{8-0.5}$, the CEB_{8-1} and the $CEB_{8-1.5}$. The main thermal properties of thermal conductivity and diffusivity were measured in the transient regime. The analysis method used is the Hot-Disk post-processing of the curves, which here considers the material as isotropic [43]. After each measurement, the system was allowed to rest for about 15 minutes to allow the initial thermal equilibrium to be restored. The tests were carried out in the laboratory at an average temperature of $24 \pm 1°C$ and a relative humidity of $40 \pm 5\%$.

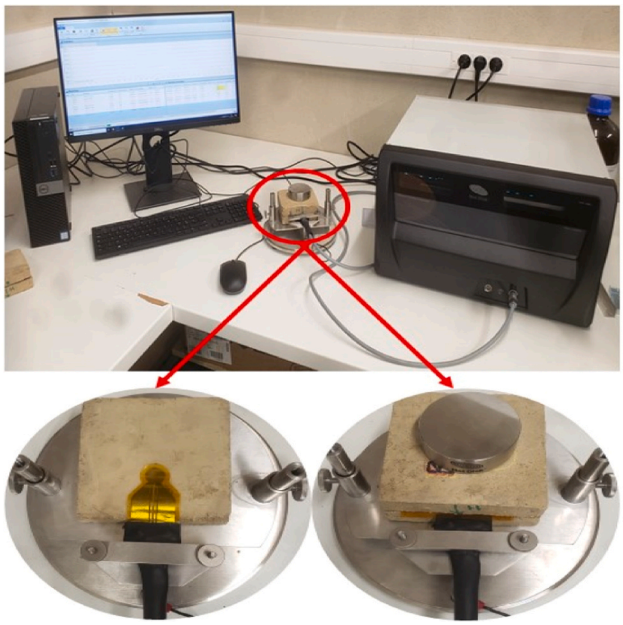

Fig. 1. Hot-disk device for measuring the thermal properties of CEBs.

2.3. Hygric characterization of clay – quackgrass straw CEBs

2.3.1. Sorption test

The sorption isotherms of the clay – quackgrass straw blocks were obtained using the gravimetric method. This approach was chosen to limit the duration of the tests. Also, according to Bui et al. [44], prolonged exposure (several weeks) of bio-sourced materials to high relative humidities, as in the case of the saturated salt solution (SSS) method, can cause deterioration of these materials (mould development) and consequently errors in the determination of sorption isotherms. For this purpose, two dynamic vapor sorption (DVS) measurement devices were used in the present study. These were the DVS Intrinsic from Surface Measurement Systems (Alperton,UK) and the V-GA2 from InstruQuest, Inc (Boca Raton, USA). The first instrument was used to determine the sorption isotherms of the main raw materials (clay and quackgrass straw) and the second instrument was used to determine the CEBs of clay and quackgrass straw respectively. The choice of two different measuring devices is justified by the limitations associated with their use. The DVS only accepts a maximum of 1*g* of the material to be tested and is therefore only suitable for materials that are assumed to be homogeneous, such as clay or quackgrass straw. The V-GA2, on the other hand, accepts a relatively large amount of material, i.e. a maximum of 100*g*, which allows a more representative volume of heterogeneous samples, such as mixtures of clay and straw, to be placed. These two instruments had demonstrated good reproducibility in a previous project (SmartReno) to characterize the sorption isotherm of some building materials. However, this required the prior calibration of the balances and the temperature and relative humidity sensors of each instrument, as well as the definition of a sufficiently stringent threshold value for the rate of change in mass with time.

To this end, 75*mg* of clay and 30*mg* of quackgrass straw were placed

Table 3
Composition and physico-mechanical properties of clay – quackgrass straw clay CEBs [35].

Samples	Composition				Physical properties		Mechanical properties
	wt% clay	*wt*% granite dust 0/5	*wt*% fibres	*wt*% cement portland	Density ($kg.m^{-3}$)	Porosity (%)	Dry compressive strength (MPa)
CEB_{8-0}	55.2	36.8	0	8	1932	27.1	5.1
$CEB_{8-0.5}$	54.9	36.6	0.5	8	1835	28.35	3.85
CEB_{8-1}	54.6	36.4	1	8	1753	31.35	2.84
$CEB_{8-1.5}$	54.3	36.2	1.5	8	1692	33%	1.76

in the DVS sample pan. The tests began with a drying phase to bring the sample to an anhydrous state. A variation of relative humidity from 0 to 90% in steps of 15 ± 0.5% was imposed for the adsorption phase and vice versa for the desorption phase. The humidity step change was conditioned by a mass balance criterion (dm/dt) defined by the weight change per minute, which had to be less than 0.0003% per 10 minutes. Equilibrium moisture content (EMC) values were determined using the last data for each tray. The sorption tests were carried out at a constant temperature of 35°C, which is about 10°C higher than that generally found in the literature. The idea was to analyse the hygric behaviour of the materials under thermal conditions representative of the humid tropical climate of southern Benin.

In addition, 26g of CEB_8 −0 and CEB_8 −1 were tested in V-GA2. To reduce the duration of the tests by increasing the specific surface area, the samples were crushed by lightly tapping the block with a hammer (Fig. 2). The size of the particles obtained was less than 0.3 cm^3. The temperature and HR sequence used to study the sorption of CEBs is identical to that used for DVS. Due to the number of samples to be tested and the time constraints, the mass equilibrium criterion was degraded this time and defined as 0.003% per 40 minutes. This criterion was refined in a previous study on cob and OSB panels to provide a good balance between test duration and quality measurement of the sorption isotherm. But, it will be seen later that this criterion makes it possible to get close to the EMC but would have deserved to be more demanding. The test was repeated for each type of material.

The tests lasted an average of one week for each CEB formulation, compared to about two weeks for the straw and one day for the clay.

2.3.2. Sorption isotherm fitting model

GAB (Guggenheim-Anderson-De Boer) is one of the most widely used models for fitting sorption isotherms of earthen building materials. Among others, it has been used by [45] to fit the sorption isotherms of corncob bioconcrete. The model was also found to be better for fitting the sorption isotherms of earth materials [46], 20th century clay bricks [47], earth blocks with agro-aggregates (alfa fibers and sawdust) [48], and date palm concrete [49]. It was therefore selected as the best model fit the sorption isotherms of CEBs in clay – quackgrass straw. As such, the fitted equilibrium moisture contents are determined by Eq. (1).

$$u = \frac{a_j.b_j.\phi}{(1-b_j.\phi)[1+(a_j-1).b_j.\phi]}.u_m \tag{1}$$

where u is the equilibrium moisture content fitted to a given relative humidity ($kg.kg^{-1}$), a_j and b_j are the fitting parameters of the GAB model, ϕ is the relative humidity (−) and u_m is the monomolecular moisture content ($kg.kg^{-1}$), i.e. the moisture content required to cover the absorbing surface with a layer of water molecules [47]. It can be determined using Eq. (2).

$$S_{GAB} = S_w.N_A.\frac{u_m}{M_1} \tag{2}$$

where S_{GAB} is the specific surface area of the sample tested (m^2), S_w is the surface area of an adsorbed water molecule (m^2), N_A is the Avogadro number ($N_A = 6,02.10^{23}\ \ mol^{-1}$) and M_1 is the molar mass of water ($M_1 = 18g.mol^{-1}$).

However, given the difficulties in determining the specific surface area of certain samples, as in the present study (crushed material), Oumeziane et al. [47] propose Eq. (3) to determine the equilibrium content fitted with the GAB model.

$$u = \frac{\phi(1-b_j)[1+(a_j-1)b_j]}{(1-b_j.\phi)[1+(a_j-1)b_j.\Phi]}.u_{sat} \tag{3}$$

Where u_{sat} is the moisture content of the saturated mass ($kg.kg^{-1}$), $m_{air,sat}$ is the mass of the water saturated sample (g) and m_0 is the mass of the anhydrous sample (g). The model parameters (a_j and b_j) are determined by the weighted least squares method.

To assess the accuracy of the models, the coefficient of determination R^2 (Eq. 4) and the sum of squares of the RSS residuals (Eq. 5) were determined. A better model fit is obtained when the R^2 is close to 1 and the sum of residuals (RSS) is low.

$$R^2 = 1 - \frac{\sum_{i=1}^{n}(u_{\exp,\ \ i} - u_{cal,\ \ i})^2}{\sum_{i=1}^{n}(u_{\exp,\ \ i} - \overline{u_{cal,\ \ i}})^2} \tag{4}$$

$$RSS = \sum_{i=1}^{n}(u_{\exp,\ \ i} - u_{cal,\ \ i})^2 \tag{5}$$

Where $u_{\exp}$ and u_{cal} are the experimental and calculated equilibrium moisture contents respectively, $\overline{u_{cal,i}}$ is the mean of the experimental equilibrium moisture contents and n is the number of experimental data.

2.3.3. Vapor permeability test

The water vapor permeability of a material reflects its ability to transfer moisture under a water vapor pressure gradient [50]. The determination of this property for the different formulations of clay – quackgrass straw CEBs was carried out using the wet cup technique in accordance with ISO standard 12572 [51]. For each formulation, three (3) cylindrical samples with a diameter of 69mm and a thickness of 21mm were used. The side surfaces of the specimens were coated with epoxy adhesive to prevent any lateral transfer of moisture during the test and to provide a smooth surface for lateral sealing. After

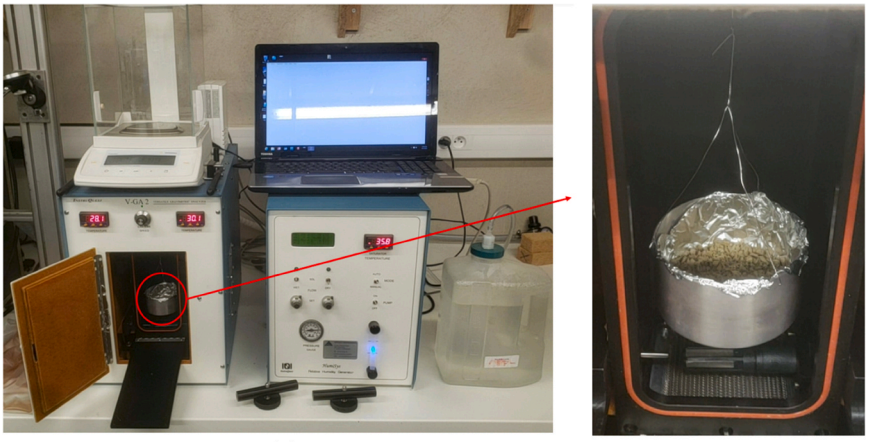

(a) (b)

Fig. 2. Test to determine sorption isotherms; (a) V-GA2 apparatus; (b) capsule containing crushed CEB.

preconditioning in a climatic chamber at 35°C and 40% humidity, the samples were placed on dishes containing a solution of sodium chloride (NaCl). The samples, whose diameter was approximately equal to the inner diameter of the beakers (Fig. 3b), were held together and sealed to the beakers using the PVC-CHA system [52].

The resulting assemblies (Fig. 3c) were placed in a climatic chamber. Using a solution saturated with sodium chloride (NaCl), a relative humidity of 75% was maintained in the cup (Fig. 3a), resulting in a partial vapour pressure gradient between the two sides of the same sample (moisture flow transfer). Each cup was weighed daily on a precision balance until the moisture flux through the material stabilised. The water vapour permeability of each sample was then determined using Eq. (6) that takes into account the resistance vapor diffusion of the air layer between the sample and the salt solution.

$$\delta = \frac{e}{\frac{S.\Delta p}{G} - \frac{e_a}{\delta_a}} \tag{6}$$

where δ is the water vapor permeability of the sample ($kg \bullet m^{-1}s^{-1}Pa^{-1}$), e is the thickness of the sample (m), S is the surface area of the sample exposed to the vapor flow (m^2), Δp is the partial vapor pressure difference across the sample (Pa), G is the flow of water vapor through the sample ($kg.s^{-1}$), e_a is the thickness of the air layer separating the sample from the saline solution (here typically $e_a = 33mm$), δ_a is the diffusion coefficient of water vapor in air ($kg \bullet m^{-1}s^{-1}Pa^{-1}$). In this case, the estimation of uncertainties was limited to the determination of standard deviations (type A uncertainty), since the accuracies of the instruments used are not all known.

The water vapor pressure difference and the water vapor permeability of the air are determined by Eqs. (7) and (8) respectively.

$$\Delta p = (HR_2 - HR_1) \times 610,5 \times e^{\left(\frac{17,269.\theta}{237,3+\theta}\right)} \tag{7}$$

$$\delta_a = \frac{2,3056 \times 10^{-5} \times p_0}{R \times T \times p}\left(\frac{T}{273}\right)^{1,81} \tag{8}$$

Where HR_2 and HR_1 are the relative humidities inside and outside the cup respectively (%), θ is the temperature (°C), p_0 is the atmospheric pressure ($p_0 = 1013,25\,hPa$), R is the perfect gas constant for water vapour ($R = 462N.M.kg^{-1}.K^{-1}$), T and p are the temperature (K) and pressure (hPa) during the test respectively.

The vapor diffusion resistance factor (μ) of the materials was calculated from Eq. (9).

$$\mu = \frac{\delta_a}{\delta} \tag{9}$$

2.4. Simulation of the hygrothermal behavior of CEBs

The properties characterized by the previous tests can be implemented in numerical simulation software for heat and mass transfer used by thermal design offices to study the hygrothermal performance of a building envelope (durability, energy consumption, etc.). However, to ensure that these numerical tools can predict the hygrothermal behavior of the eco-material used in this study, the models have to be validated experimentally.

The software used for the measurement-prediction comparison is Wufi6 (IBP, Fraunhofer Institute, Germany). A description of this tool can be found in [53].

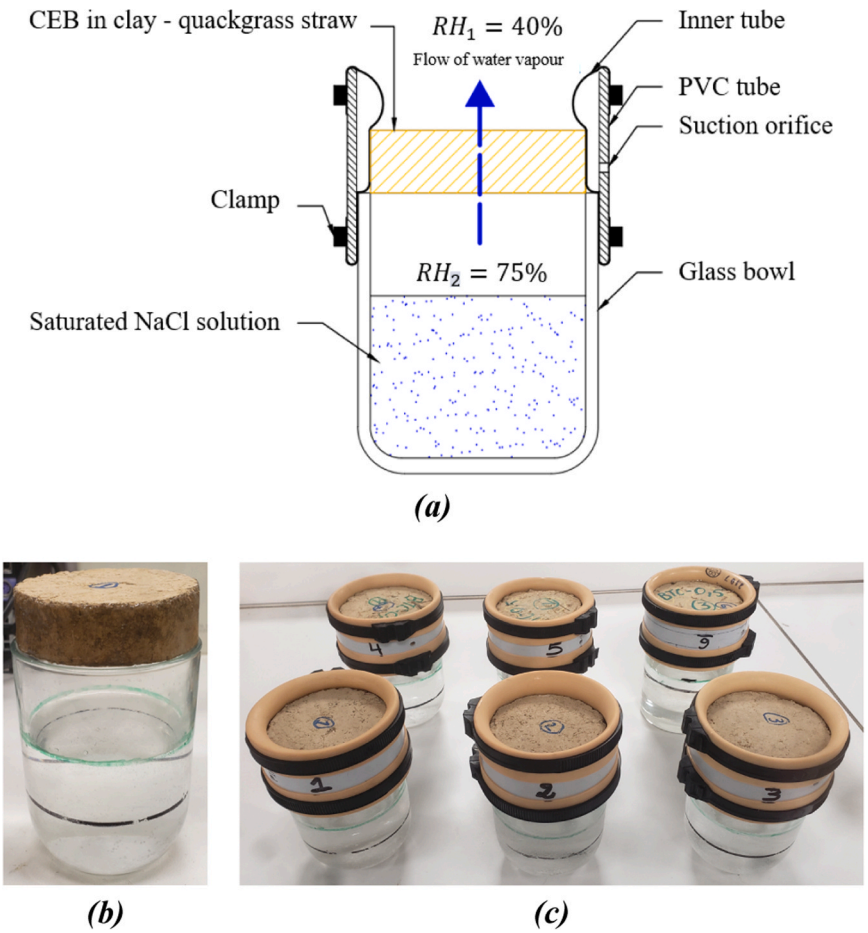

Fig. 3. (a) Descriptive diagram of the cup-sample-PVC-CHA assembly; (b) sample not yet sealed on the cup; (c) Cups and sample holding systems.

The hygrothermal behavior of CEBs made of clay and quackgrass straw was tested by subjecting the material to variable hygrothermal conditions at the exchange surfaces and by monitoring changes in temperature and relative humidity (RH) at the core of the material. The aim of this test was to approximate some sequences of climatic conditions to which building envelope materials are exposed, and then to compare measurements and simulations in order to validate the ability to predict the hygrothermal behavior of these materials.

The experiment consisted of inserting a Hygro-Button from Plug and Track (Willems, France) into a sample of the material under investigation to measure changes in temperature within it. A Hygro Button is an autonomous compact data logger (6*mm* thick, 16*mm* of diameter) with no wired connection designed to monitor RH and temperature. To do this, two samples of clay – quackgrass straw of the same formulation and measuring $10 \times 10 \times 2$ cm^3 were assembled and held together with aluminum tape (Fig. 4.b). A small pocket was made in the centre of the contact surface of one of the samples to house a hygro-button (Fig. 4.a). The samples were preconditioned at $35°C$ and 40% RH for 36 hours before the hygro-buttons were applied. The contact surfaces of the two samples were assumed to be sufficiently flat to ensure perfect contact. Only formulations CEB_8-0 and CEB_8-1 were included in these validation tests. For each of the formulations, two assemblies (samples + hygro-button) were carried out.

The resulting assemblies were placed in a climate chamber (Memert HPP 260) where the temperature and humidity scenario shown in Fig. 5 was run. This scenario is identical to that employed in the simulations. Initially, the temperature and RH were set at $35°C$ and 40% respectively for approximately three hours. This was followed by a $15°C$ increase in temperature for 17 hours and the RH was maintained at the initial value. This first phase made it possible to study the thermal behaviour of the material alone under temperature variation. This was followed by a simultaneous variation of both parameters, temperature and RH, reducing the temperature from $50°C$ to $35°C$ and increasing the relative humidity from 40% to 80% for 9 hours. Finally, the temperature was reduced to $28°C$ while the humidity was reduced in two steps, to 60% after 21 hours and then to 50%. The aim of this final stage was to study moisture transfer within the material under isothermal conditions. A hygro button was placed in the climate chamber to measure the actual hygrothermal conditions in the chamber. The time step for recording was 2 minutes. The changes in temperature and humidity measured in this way are also shown in Fig. 5. The difference between the conditions set and those measured in the climatic chamber is sometimes significant. Regulation overshoot at setpoint changes, cooling difficulties or power failure at 30 hours are observed in Fig. 5. The hourly averages of temperature and RH measured in the climate chamber are used as input data for the WUFI simulations.

Statistical indices such as mean bias error (*MBE*), root mean square error (*RMSE*) and coefficient of variation of the root mean square error ($CV(RMSE)$), defined by Eqs. (10), (11) and (12) respectively, were calculated to evaluate the accuracy of the simulation results. Simulation results are considered accurate when the *MBE* is ±10% and the $CV(RMSE) \leq 30\%$ using hourly data.

$$MBE = \sum_1^n \left(y_{sim,\ \ i} - y_{\exp,i}\right) \Big/ \sum_1^n y_{\exp,i} \times 100 \tag{10}$$

$$RMSE = \sqrt{\sum_1^n \left(y_{sim,\ \ i} - y_{\exp,i}\right)^2 \Big/ n} \tag{11}$$

$$CV(RMSE) = RMSE \Big/ \overline{y_{\exp}} \times 100 \tag{12}$$

Where n is the number of simulated or experimental data (−), $y_{sim,i}$ is the simulated temperature ($°C$) or relative humidity (%), $y_{\exp,i}$is the experimental temperature ($°C$) or RH (%) and $\overline{y_{\exp}}$ is the mean of the experimental temperature ($°C$) or relative humidity (%).

3. Results and discussion

3.1. Thermal properties

At the end of the thermal characterisation tests, the thermal conductivity obtained for the control material at 40% relative humidity ($CEB_8 - 0$) is $0.74 W.m^{-1}.K^{-1}$. This value is lower than $0.8 W.m^{-1}.K^{-1}$, $0.84 W.m^{-1}.K^{-1}$, $0.85 W.m^{-1}.K^{-1}$, $0.96 W.m^{-1}.K^{-1}$, $1.46 W.m^{-1}.K^{-1}$, $1.7 W.m^{-1}.K^{-1}$ and $2 W.m^{-1}.K^{-1}$ obtained by [26,54-58] and [27] for the same types of materials. However, it is higher than the control CEB thermal conductivities of Zhang et al. [10] ($\lambda = 0.52 W.m^{-1}.K^{-1}$) and Laborel Préneron at al. [12] ($\lambda = 0.57 W.m^{-1}.K^{-1}$). The observed discrepancies can be attributed to the measurement techniques employed in each study, the nature of the soils, and the density and porosity of the CEBs considered. In fact, the denser a material, the fewer pores it contains and therefore the smaller the volume of air that can slow down heat transfer within it ($\lambda_{air} = 0.026 W.m^{-1}.K^{-1}$). As proof of this, Ben Mansour et al. [49] have demonstrated the linear relationships existing between the thermal conductivity, density and porosity of a CEB. According to this study, for a compaction pressure of between 0.39 and 3.16*MPa*, the density and porosity of the material vary respectively from 1610 to $2194 kg.m^{-3}$ and from 41.6 to 21.7%. These variations justify the increase in thermal conductivity from 0.618 to $1.483 W.m^{-1}.K^{-1}$.

Furthermore, the effect of quackgrass straw on the thermal conductivity of the soil matrix is shown in Fig. 6. A slight decrease in conductivity can be observed when the amount of straw incorporated is between 0 and 1% of the mass of the soil matrix. The values obtained for $CEB_8-0,5$ and CEB_8-1 are $0.72 W.m^{-1}.K^{-1}$ and $0.70 W.m^{-1}.K^{-1}$ respectively, i.e. slight reductions of 2.7% and 5.4%. For similar proportions, Taallah & Guettala [56] obtain a 10.6% reduction in the thermal conductivity of their CEB with only 0.2% date palm fibre. This reduction reaches 20% when Ajouguim et al. [58] incorporate 1% Alfa fibre in the soil matrix. The same is true for Laibi et al. [27], who found a reduction of around 30% with 1.2% kenaf fibre. Ashour et al. [57] obtained reductions of about 36% when using 1% barley straw and wheat

(a) (b)

Fig. 4. (a) Sample with hygro-button; (b) Sample + hygro-button assembly.

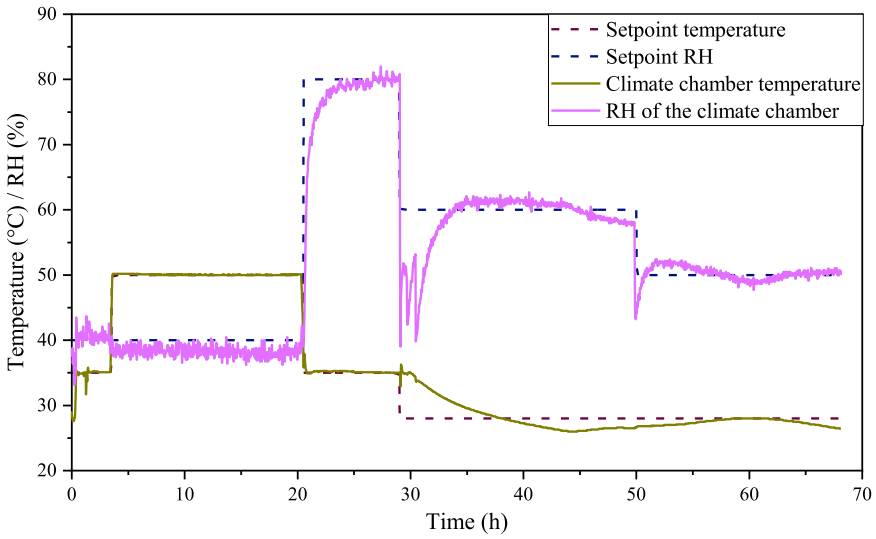

Fig. 5. Hygrothermal validation scenario.

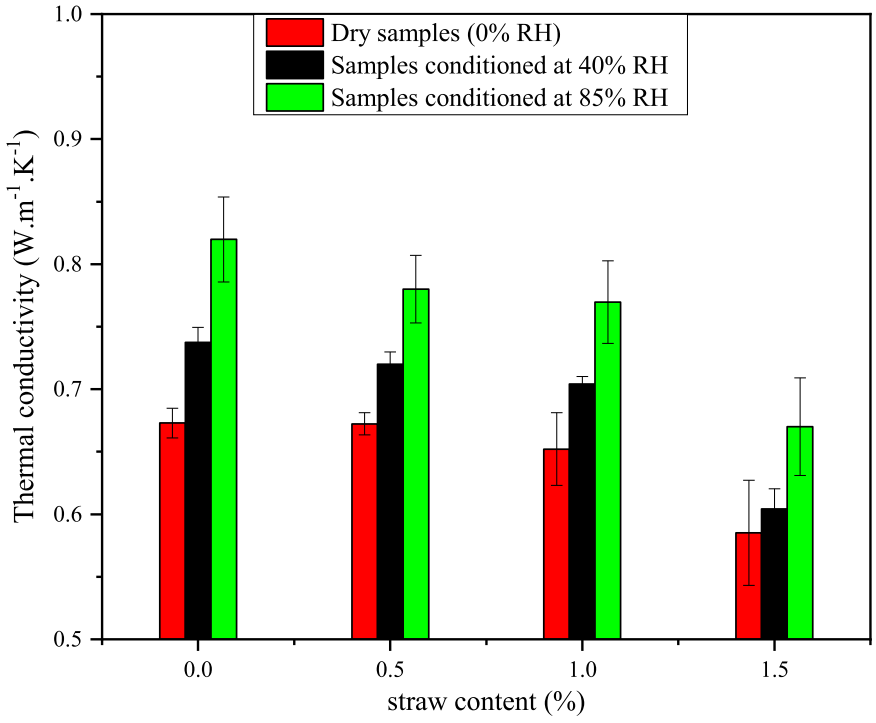

Fig. 6. Thermal conductivity of CEBs at different relative humidities.

straw, reducing the thermal conductivity of fibre-free blocks from $0.96W.m^{-1}.K^{-1}$ to $0.59W.m^{-1}.K^{-1}$ and $0.62W.m^{-1}.K^{-1}$, respectively. These differences between the literature values and those of the present study can be explained by the dimensions of the fibres used and their proportion in relation to the amount of binder, the degree of compaction and the induced interparticle porosity [59]. It has been established that the presence of biosourced fibres (which are generally more porous) in the earth matrix increases the porosity of the material. Depending on their length, these fibres also encourage the creation of air pockets by reducing contact between the earth particles, making the materials more thermally insulating. However, a reorganization of the particles can be observed as a function of the compacting pressure of the blocks, thus affecting the pore network and consequently the thermal conductivities of the materials.

Furthermore, by subjecting the samples to a RH like the average observed in the humid tropical climate of southern Benin (RH_{moy} = 85%), an increase in thermal conductivity is observed for all the formulations. Conductivities of $0.82W.m^{-1}.K^{-1}$, $0.78W.m^{-1}.K^{-1}$, $0.77W.m^{-1}.K^{-1}$ and $0.67W.m^{-1}.K^{-1}$ are measured for $CEB_8 - 0$, $CEB_8 - 0.5$, CEB_8 −1 and CEB_8 −1.5 respectively (Fig. 6). Compared to the thermal conductivities of CEBs in the anhydrous state, the increases obtained at 85%*RH* are 22.4%, 16.4%, 18.5% and 15.5% respectively. This can be explained by a general increase of about 3% in the water content of the samples as the RH increases from 0% to 85%, water being more conductive than air (λ_{eau} = $0.595W.m^{-1}.K^{-1}$). Despite these increases, the values obtained are in line with those reported in the literature [54, 55] and are well below the thermal conductivity of conventional concrete blocks used in building envelopes ($1.7W.m^{-1}.K^{-1}$[11]). An

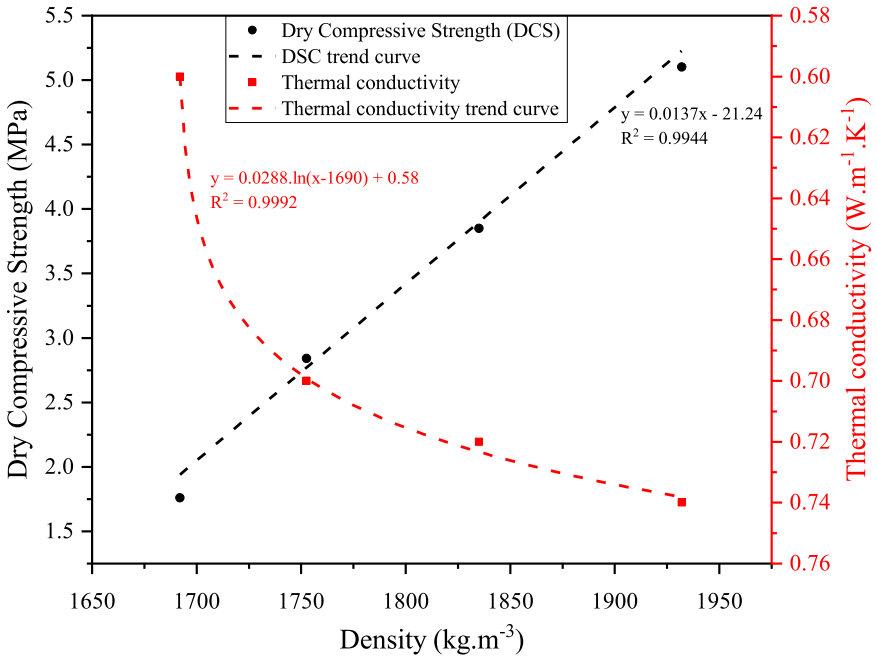

Fig. 7. Selection of a formulation that is thermally and mechanically efficient.

analysis of the thermal behavior of clay – quackgrass-straw CEBs as a function of straw and moisture content allows us to confirm that they are more sensitive to moisture than quackgrass straw. For instance, the thermal conductivity of CEB_8-0 changes by approximately 23% at only 85%*RH*, compared to an increase of 19% in the presence of 1.5*wt*% quackgrass straw. This therefore supports the claim by Costantini Romero et al. [60] that earthen materials are thermally more sensitive to moisture.

It appears obvious that the use of quackgrass clay CEBs in the construction of building envelopes would generate a passive enhancement of thermal comfort through better thermal insulation of building.

Table 4 shows all the thermal properties of the different formulations of CEB clay – quackgrass straw at 40% relative humidity. From the analysis of the data in this table, the $CEB_8-1.5$ appears to be the most suitable material for significantly reducing the energy consumption of buildings. It has a lower thermal conductivity and therefore the best ability to limit heat transfer within it. Its slightly higher thermal capacity and lower thermal diffusivity allows it to slow down the rate of heat propagation in transient conditions. This gives it good thermal inertia. However, this formulation cannot be used because its mechanical properties (low compressive strength) make it unsuitable for use in building envelopes ($DCS < 2MPa$) [35]. Therefore,$CEB_8 - 1.5$, whose dry and wet compressive strengths were two low, with 1.76 MPa and 0.56 MPa respectively [35], was not retained. In other words, increasing the content of plants aggregates in clay matrices improves the thermal performance of composites at the expense of their mechanical performance. This was indeed observed by Ben Mansour et al. [49]. A compromise between thermal and mechanical performance led the authors to consider $CEB_8 - 1$. This result justifies the choice of this formulation as the only quackgrass straw material to have undergone the sorption and vapour permeability tests.

3.2. Hygric properties

3.2.1. Sorption isotherms Raw materials

Analysis of the plots shows that the equilibrium criterion set for these tests ($dm/dt = 0.0003\%/10\text{min}$) is met, as hygrometric equilibrium is reached within the materials before any change in humidity. The sorption results for the two materials (Fig. 8) show that, logically, the quackgrass straw adsorbs significantly more moisture than the clay. At 90%*RH*, the corresponding equilibrium moisture content (EMC) of clay and quackgrass straw is 6.4% and 24.2% respectively. A comparison with the soil studied by Laborel-Préneron et al. [12] shows that the EMC reached by the Zogbodomey clay at 90%*RH* is about three times higher. However, the dominant presence of kaolinite in Zogbodomey clay (> 50%) [35] affects the adsorption rate. According to Liuzzi et al. [14], kaolinite is relatively less sensitive to moisture than other clay minerals such as montmorillonite and illite. This is confirmed by the work of Cagnon et al. [13] who, after determining the sorption isotherms of five clay bricks of different mineralogy, observed that only the brick composed mainly of kaolinite absorbed half as much moisture as the other four, composed of a mixture of illite, chlorite and montmorillonite.

As for quackgrass straw, its relatively high EMC reflects the hygroscopic nature of the material. Based on the literature consulted, the EMC at 90%*RH* of quackgrass straw (24.2%) appears to be higher than that of other plant aggregates. For instance, in sorption tests carried out at 25°*C* at DVS by Hill et al. [61], the moisture contents at 90%*RH* of jute, coir, flax, Sitka spruce, hemp and cotton fibres are approximately 20, 22, 16, 19.5, 19 and 12% respectively. These contents are 19% for hemp chips, 23% for corn on the cob and 22% for barley straw at 90%*RH* and 23°*C* [12]. For the latter aggregate, Bui et al. [44] analyzed the sorption isotherms of the material obtained by the saturated salt solution (SSS) and DVS methods. They concluded that both approaches gave similar

Table 4
Thermal properties of different formulations of CEB clay - quackgrass straw at 40% relative humidity.

Sample	ρ (kg.m^{-3})	DCM (MPa)	λ (W.m^{-1}.K^{-1})	a (mm^2.s^{-1})	C_p (J.kg^{-1}.K^{-1})	E (W.K^{-1}.m^{-2}.s$^{-0.5}$)
$CEB_8 - 0$	1932 ± 6	5.1 ± 0.5	0.74 ± 0,02	0.59 ± 0,08	633 ± 34	951 ± 88
$CEB_8 - 0.5$	1835 ± 3	3.85 ± 1,1	0.72 ± 0,02	0.60 ± 0,11	682 ± 16	952 ± 124
$CEB_8 - 1$	1753 ± 7	2.84 ± 0,9	0.70 ± 0,03	0.57 ± 0,07	729 ± 64	962 ± 58
$CEB_8 - 1.5$	1692 ± 5	1.76 ± 0,2	0.60 ± 0,04	0.61 ± 0,19	785 ± 9	942 ± 48

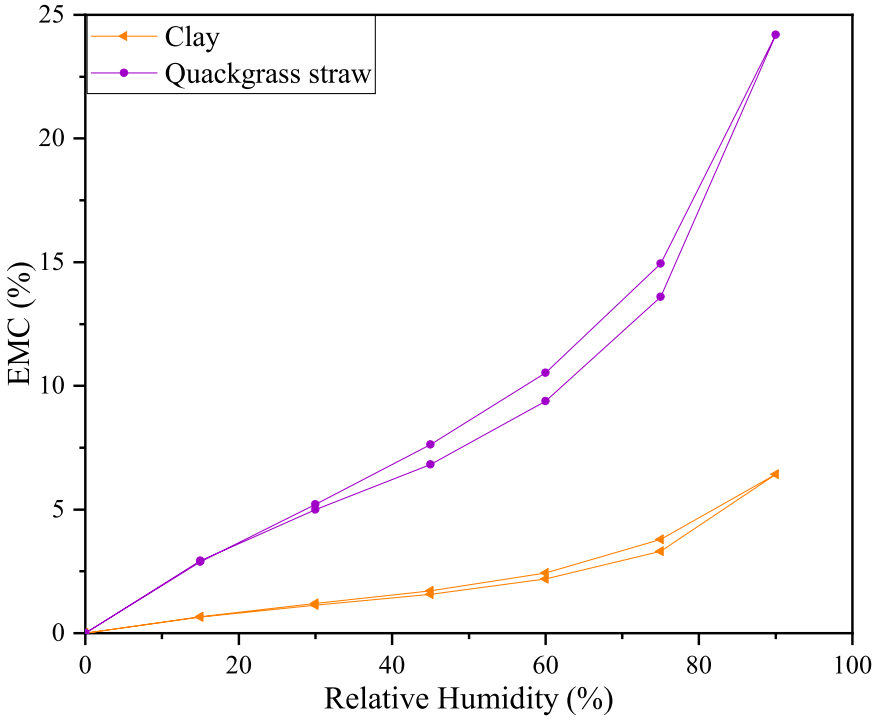

Fig. 8. Sorption isotherms at 35°*C* for clay and quackgrass straw.

sorption isotherms, with an equilibrium moisture content of 20% at 90% *RH* and 23°*C*. Whilst it is true that the comparative data were obtained at temperatures approximately 10°*C* lower than that used in the present study (35°*C*), it should be noted that increasing temperature reduces the adsorption rate of bio-based materials [62]. It can therefore be concluded that quackgrass straw is more hygroscopic than most bio-based materials incorporated into soil matrices. Therefore, incorporation of quackgrass straw into the soil matrix should improve the sorption capacity of the material.

The hysteresis between the adsorption and desorption curves is present for both materials, but remains very low, $<$ 2% at most in the central part (between 40% and 75%*RH*).

❖ CEB clay - quackgrass straw

According to the results of the thermal characterization, CEB_8-1

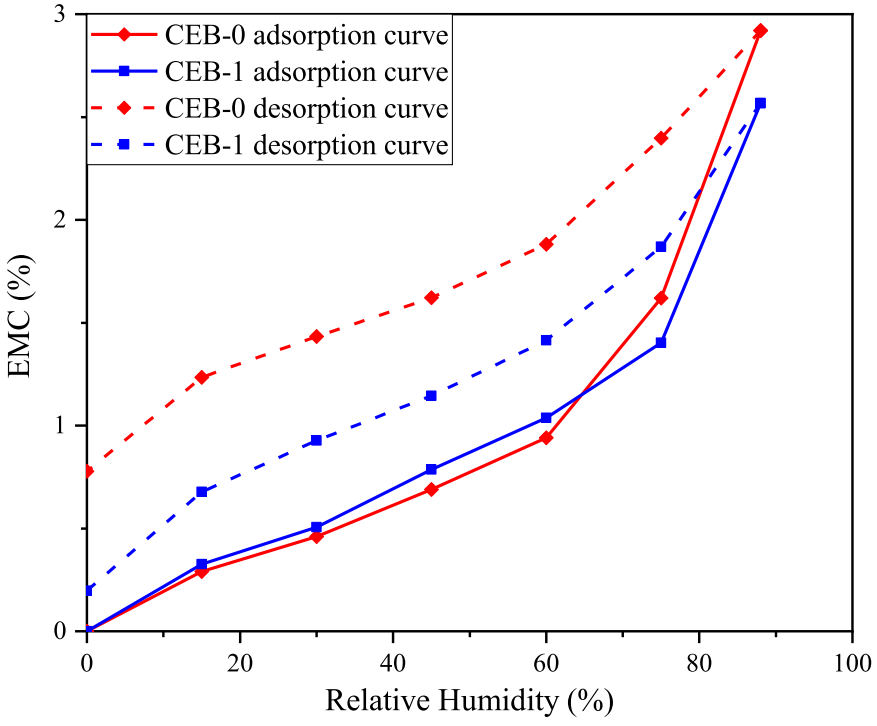

Fig. 9. Sorption curves for CEB_8-0 and CEB_8-1.

was found to be the most effective formulation given the thermo-mechanical constraints (Fig. 7). For this reason, the determination of sorption isotherms was mainly focused on CEB_8 − 1. However, to assess the influence of quackgrass straw on the sorption capacity of the soil matrix, the sorption isotherms of CEB_8 −0 were also determined.

It should be noted that it would be necessary to tighten the equilibrium criterion below 0.003%/40 min. The shapes of the mass curves have showed that the samples clearly do not reach mass equilibrium at the end of each RH step (Appendix A). This is particularly noticeable when the RH is above 40%, where an error occurs in the estimation of the asymptotic mass at each RH step. Fig. 9 shows the sorption curves, which can only be considered as very approximate since the equilibrium criterion is not sufficiently demanding. This may have led to an underestimation of the true hygroscopicity of the material. It is also observed that the EMC at the end of the adsorption-desorption cycle has an irreversible dynamic with an offset due to chemisorption phenomena during the cycle. This has been observed by Nils Frantz [59] for hemp-lime concretes in tests lasting several months. The lack of equilibrium in certain compositions was attributed to the binder, which certainly had not completed all the setting reactions in the concrete due to insufficient water during production. During adsorption, high moisture levels can trigger delayed reactions with concrete, leading to progressive mass fixation. Nils Frantz [59] observed that the offset is more or less pronounced depending on the intensity of compaction and the binder/particle ratio chosen during production, as they influence the availability of water to the binder and the migration of water through the inter- and intra- binder/particles. Other studies on hemp concrete [63,64] confirm the presence of hysteresis phenomena, with an irreversible mass gain during adsorption, resulting in an offset during desorption.

The adsorption curves for the two formulations correspond to a Type II isotherm according to the IUPAC classification. This classification provides information on the macroporous structure of the blocks. Further analysis of the sorption curves reveals the EMC of the samples over a RH range of 0 − 60%. The maximum content reached in this range is 0.93% for CEB_8 −0 and 1.03% for CEB_8 − 1. However, beyond this range, the equilibrium moisture contents of the samples change rapidly, doubling or even tripling at only 88%*RH*. This behavior of the materials may be due to the binder not having fully reacted as discussed above, but also to the analysis of Hansen et al. [65] that earthen materials absorb much more moisture at high RH, generally above 90%.

Thus, at 88%*RH*, the equilibrium moisture content of the CEB_8 −0 is 2.92%, less than half the initial EMC of the bulk clay. Such a reduction in the sorption capacity of the blocks can be justified by the replacement of a large proportion (around 36*wt*%) of the clay by a material with very low hygroscopicity (0/5 granite dust). The addition of cement is also a significant cause. According to Saidi et al. [66], the use of chemical stabilisers in earth materials reduces their adsorptive capacity. The authors showed that the $EMC_{97\%}$ of their CEBs decreases from 5.69 to 3.7% when the cement content increases from 0 to 12%. The EMC obtained by the authors at 88%*RH* with 0% and 8% cement are 4.5% and 3.4% respectively. Still with 8% cement and at 88%*RH*, McGregor et al. [67] observed a 22% reduction in EMC compared to unstabilised earth blocks. In these two studies a similar behaviour of the materials was observed in the presence of lime. In some of the works consulted, the EMCs determined for earth materials are higher than those for CEB_8 −0 [57,66]. In addition to the influence of the 0/5 granite dust, these discrepancies may again be related to the temperature difference between the sorption tests. As with the raw materials, the sorption isotherms of CEB_8 −0 and CEB_8 −1 were determined at 35°*C*, whereas this temperature generally varies from 23 to 25°*C* in the literature; this may partly explains the lower values obtained with the clay – quackgrass straw blocks. Furthermore, Daian [68] states that the EMC of building materials decreases with increasing temperature. In this sense, Ashour et al. [57] observed a 16% decrease in the average EMC of their clay blocks when the temperature increased from 10 to 40°*C*. The authors were also interested in the influence of plant fibers on the sorption dynamics of CEBs. At 40°*C*, a general increase in the EMC_{moy} was observed after the addition of 1% and 3% wheat straw. In contrast, for the same levels of barley straw, the *EMC* decreased by 2.4% and increased by 3.8%, respectively. Less similar behavior was observed with CEB_8 − 1.

Indeed, in the RH interval [0%, 60%], the *EMC* of the soil matrix increases by about 13% after the addition of 1% quackgrass straw. Beyond this interval, however, there is a change in trend. The *EMC* of CEB_8 −1 decreases by 12.77%, resulting in a moisture content of 2.92% for the CEB_8 −0 compared to 2.57% for the CEB_8 − 1. However, a more detailed analysis of this trend is difficult due to the insufficiently demanding balance criterion. In addition, the offset after one sorption cycle observed at 0%*RH* for CEB_8 −0 is relatively larger than that for CEB_8 −1 (Fig. 9).The concrete setting reactions would be more advanced for the CEB_8 −1 composition, possibly due to the moisture input from the plant fibres. However, again, further analysis would be required to better identify the cause and with a more demanding balance criterion.

3.2.2. Fitting of CEB Sorption Isotherms

Fig. 10 shows the fitting of the sorption isotherms of CEB_8 −0 and CEB_8 −1 with the GAB model. The coefficients a_j and b_j used for this purpose are shown in Table 5. In the same table the statistical indices of the model accuracy are shown. In general, a good fit of the sorption isotherms was observed. The desorption curve was not analysed with the GAB model because of the observed offset and the chemisorption phenomena observed during the adsorption-desorption cycle. The coefficients of determination (R^2) and the residual sums of squares (*RSS*) vary from 0.97 and $1.24.10^{-5}$ to $1.451.10^{-5}$ respectively. This demonstrates the good ability of the GAB model to predict the adsorption behaviour of CEBs in clay – quackgrass straw. These values are close to the fitting results described as excellent by [48], for which the statistical accuracy indices R^2 and *RSS* are of the order of 0.999 and $0.848.10^{-5}$, respectively.

The theoretical equilibrium moisture contents obtained with this model at 95%*RH* are 5.1% and 5.5% for CEB_8 −0 and CEB_8 −1 respectively. From 88%*RH* to 95%*RH*, a clear improvement in the sorption capacity of CEBs can be observed, confirming the very good sorption capacity of earthen materials in environments with high RH. In addition, the use of clay – quackgrass straw CEBs in a humid tropical climate such as that of southern Benin would therefore contribute to the passive control of humidity in buildings, thus improving energy efficiency by reduction of dehumidification loads and maintaining the hygrothermal comfort of the occupants.

3.2.3. Water vapor permeability

The values obtained for the water vapor permeability using the cup method are 0.92×10^{-11}kg.m^{-1}.s^{-1}.Pa^{-1} and 1.16×10^{-11}kg.m^{-1}.s^{-1}.Pa^{-1} respectively for quackgrass straw contents of 0 and 1*wt*%. These values are relatively low for soil materials. However, they can be explained by the presence of 36*wt*% 0/5 granite dust in the soil matrix, which reduces its porosity. This hypothesis is supported by the work of Jraba et al. [69], who obtained vapour permeabilities ranging from 1.01×10^{-11} to 1.15×10^{-11}kg.m^{-1}.s^{-1}.Pa^{-1} with CEBs of similar composition (70*wt*% soil, 30*wt*% crushed sand and 0 to 1*wt*% Posidonia fibres). However, the influence of the cement on the permeability values obtained cannot be neglected. In fact, [70] states that the addition of cement to earthen materials makes them denser, with a consequent reduction in their vapour permeability. There are differing opinions in the literature on this point. For example, vapour permeability tests carried out by [14] on unstabilised earth materials of different mineralogical composition and those stabilised with 5% lime show opposite trends. For some samples, the permeability decreases from 2.2×10^{-11} to 2.08×10^{-11}kg.m^{-1}.s^{-1}.Pa^{-1} with the incorporation of lime, while for others it increases from 2.12×10^{-11} to 2.41×10^{-11}kg.m^{-1}.s^{-1}.Pa^{-1} and from 1.7×10^{-11} to 2.05×10^{-11}kg.m^{-1}.s^{-1}.Pa^{-1},

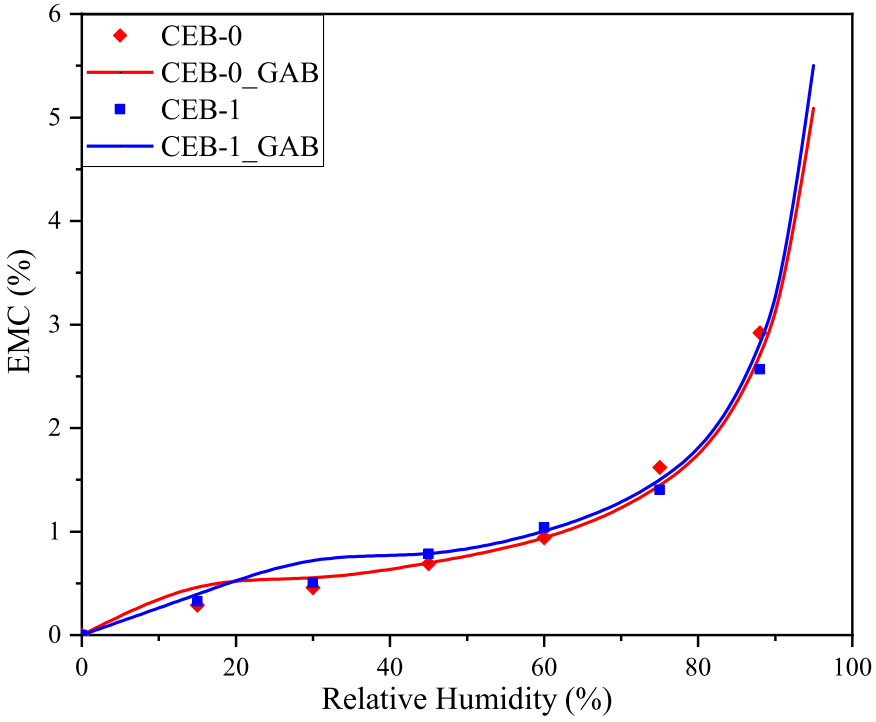

Fig. 10. Adjusted adsorption isotherms for CEB_8-0 and CEB_8-1.

Table 5
Parameters used to fit adsorption isotherms with the GAB model.

	GAB model parameter		Statistical parameters precision	
Adsorption	a_j	b_j	R^2	RSS ($.10^{-5}$)
CEB_8-0	0,99865	719,38461	0,97437	1,45112
CEB_8-1	0,90812	10,65041	0,97166	1,2453

respectively. In the tests by McGregor et al. [67], the water vapor permeability developed in the opposite direction to the chemical binder content (cement and lime). In addition, it can be seen that the incorporation of 1% quackgrass straw (a porous material) improves the permeability of CEB_8-0 by about 20%.

The corresponding vapor diffusion resistance factors (μ) orresponding to CEB_8-0 and CEB_8-1 are 21.8 and 17.4 respectively. Although the μ of the CEBs for clay – quackgrass straw are in the same order of magnitude as those of [69] (18.74 to 15.64), they are relatively higher than those obtained for certain biocomposite earth materials in the literature consulted. This is the case of Laborel-Préneron et al. [12], who obtain resistance factors between 4.8 and 7. These factors range from 5.5 to 8.8 and from 7 to 8 respectively for the CEBs used by McGregor et al. [67] and Touré et al. [71].

3.3. Hygrothermal behavior of CEBs

3.3.1. Experimental results

Figs. 11a and 11b show the evolution of temperature and RH within the materials. It should be noted that hygrothermal behavior of the tested samples was nearly identical for the same formulations. The slight discrepancies are within the measurement uncertainty of the hygrobuttons. Therefore, for each formulation only one sample is represented.

To facilitate the comparison between the hygrothermal behavior of CEB_8-0 and CEB_8-1 and later with simulations, the hourly averages of the measurements have been used in Fig. 11. Both types of samples have almost identical thermal behaviour (Fig. 11a). This is due in part to the small difference between the thermal conductivities of the two materials (around 6%) at both 40%*RH* and 85%*RH*. However, despite the small variation in moisture sorption and vapour permeability properties between the materials as a function of straw content, the CEB_8-1 is more sensitive to moisture variations (Fig. 11b). When the RH in the chamber is suddenly increased at 20 h from 40% to 80%, the RH at core of CEB_8-1 increases from 40% to 54% in 14 hours, while that of CEB_8-0 increases from 39% to 48% in the same period. This difference of about 5%*RH* cannot be attributed to the accuracy of the hygrometers, since their reliability was proven at the beginning of the experiment (similar hygric behaviour of the samples at 40%*RH*). There is also a time lag of about 2 hours at the start of the RH increase in the two samples. In addition, the change from 80% to 60% RH in the chamber at around 30 h induces a change in the slope of the increase in RH at core, again with a time lag. At the final stage, around 50 h, the 10% loss of RH in the climatic chamber caused a slight drop in RH in CEB_8-1. It therefore seems clear that the presence of Chindent straw in the soil matrix promotes the material's reactivity to moisture. This could be an advantage for the passive control of the RH of indoor environments.

3.3.2. Comparison of simulations results and measurements

Figs. 11a and 11b compare the measured and simulated temperature and humidity trends within CEB_8-0 and CEB_8-1 respectively. The time constant of the temperature change at core is faster for the measurement than for the simulation (Fig. 11a). In fact, the geometry of our samples certainly does not allow to be in a one-dimensional heat transfer configuration along the thickness, as assumed by the Wufi software. Overall, a good agreement between the simulated and measured data can be observed. This is demonstrated by the fact that the calculated statistical indices are relatively close to 0 (Table 6). The mean bias errors (*MBE*) for the CEB_8-0 are 0.95% for temperature and -0.36% for RH. These values are 0.36% and 1.96% respectively for the CEB_8-1. As for the root mean square error ($CV(RMSE)$), they vary between 2.54% and 2.76%. All these values are well below the recommended thresholds (± 10 for *MBE* and 30% for $CV(RMSE)$), which demonstrate the accuracy of the simulation results. All this confirms the reliability of the hygrothermal properties of the clay – quackgrass straw CEBs determined above and of the good ability of the WUFI software to simulate the hygrothermal behaviour of the materials of this work.

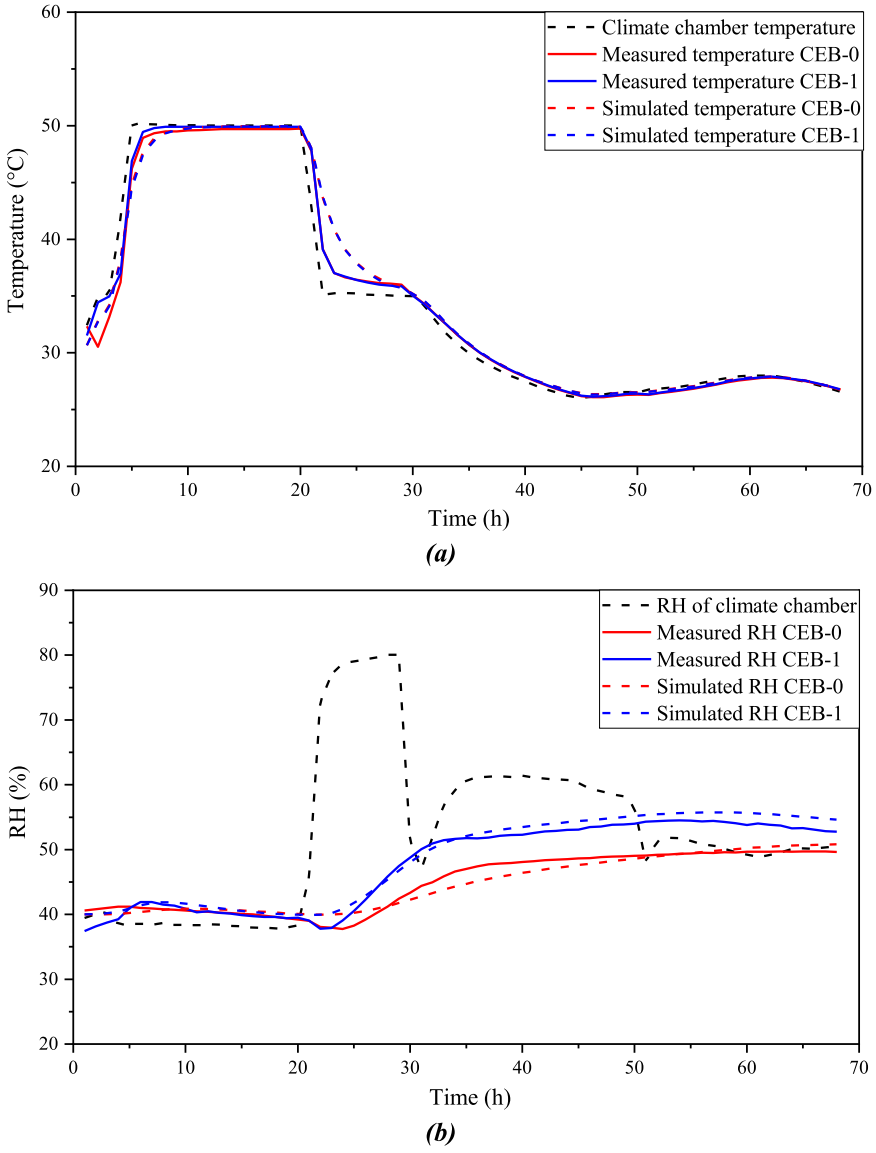

Fig. 11. Comparison between experimental and simulated behavior of CEB_8 −0 and CEB_8 −1 (a) temperature; (b) RH.

Table 6
Statistical indices for the comparison measurements simulations results.

Statistical index	$CEB_8 - 0$		$CEB_8 - 1$	
	Temperature	RH	Temperature	RH
MBE (%)	0.95	− 0.36	0.36	1.96
RMSE	0.96	1.15	0.96	1.21
CV(RMSE) (%)	2.76	2.56	2.75	2.54

4. Conclusion

This paper investigates the hygrothermal properties of compressed earth blocks made of clay and quackgrass straw. The material consists of an earth matrix (clay + 0/5 granite dust), 8*wt*% cement and 0 to 1.5*wt*% quackgrass straw in increments of 0.5. Thermal characterisation tests carried out on the materials ($CEB_8 - 0$, $CEB_8 - 0.5$, $CEB_8 - 1$, and $CEB_8 - 1.5$) in the present paper showed a decrease in thermal conductivity at different relative humidities with increasing quackgrass straw content. The oven-dry conductivities obtained for these four formulations range from 0.58 to $0.67 W.m^{-1}.K^{-1}$. At 40%*RH*, these values increase and are in the range of 0.6 to $0.74 W.m^{-1}.K^{-1}$ and then 0.67 to $0.82 W.m^{-1}.K^{-1}$ at 85%*RH*. A comparison between the contents of straw and moisture reveals that moisture has a greater effect on thermal conductivity, both moving in the same direction. However, the thermal conductivities obtained remain lower than those of conventional materials. In addition, since the improvement in the thermal properties of clay-couch grass straw CEBs is at the expense of their mechanical properties, the results show that the addition of 1 % quackgrass straw to the clay matrix ($CEB_8 - 1$) represents a good compromise.

Furthermore, the hygric characterization of these materials revealed an equilibrium moisture content of 2.92% at 88%*RH* at 35°*C* for $CEB_8 - 0$, followed by a vapor permeability of $1.16 \times 10^{-11} kg.m^{-1}.s^{-1}.Pa^{-1}$. These values are 2.57% and $0.92 \times 10^{-11} kg.m^{-1}.s^{-1}.Pa^{-1}$ respectively for $CEB_8 - 1$. Taken together, these results demonstrate the ability of clay – quackgrass straw CEBs to improve the energy performance of buildings and the hygrothermal comfort of occupants through better thermal insulation of the envelope and passive control of indoor humidity.

In addition, the heat transfer experiments conducted on CEB_8 −0 and CEB_8 −1 demonstrate analogous thermal behaviour between the two material types. However, a greater sensitivity to variations in relative humidity is obvious in $CEB_8 - 1$, likely attributable to the incorporation

of quackgrass straw. In comparison with the results of the simulations performed in Wufi, a similarity between the experimental data and the simulated data is apparent. The minor discrepancies observed, particularly between the experimental and simulated moisture profiles, can be attributed not only to the precision of the hygro-buttons, but also to the limitations of the simulation. These include the assumption of homogeneity of the clay – quackgrass straw CEBs, the unidirectional transfer of heat and moisture through the material's thickness, and the fact that the experimental desorption isotherms were not considered in the simulation model. Despite this, it can be concluded that the Wufi software captures the transient hygrothermal behaviour of quackgrass straw CEBs with a reasonable degree of accuracy. This provides a solid foundation for simulating the hygrothermal behaviour of the material at building scale and for assessing its energy performance.

CRediT authorship contribution statement

André Philippe: Writing – review & editing, Supervision, Project administration, Funding acquisition, Conceptualization. **HOUNGAN Aristide Comlan:** Writing – review & editing, Visualization, Funding acquisition. **Rémond Romain:** Writing – review & editing, Supervision, Methodology, Investigation, Conceptualization. **KIKI Gratien Jesugo:** Writing – review & editing, Writing – original draft, Methodology, Investigation, Conceptualization. **Ouertani Sahbi:** Methodology, Investigation.

Declaration of Competing Interest

The authors declare that they have no known competing financial interests or personal relationships that could have appeared to influence the work reported in this paper

Acknowledgements

The authors gratefully acknowledge the financial support of Académie de Recherche et d'Enseignement Supérieur (ARES) of Fédération Wallonie-Bruxelles (FWB).

Appendix A. Mass change during sorption isotherm characterisation

Figure A.1 shows the sequence of relative humidity applied and sample mass change for DVS-intrinsic (a) and V-GA2 (b). The mass rate at the end of each RH step shows a constrasting equilibrium criterion, 0.0003%/10min for the first and 0.003% / 40 min for the second apparatus. The example shows the mass evolution for clay (a) and for the formulation $CEB_8 - 1$.

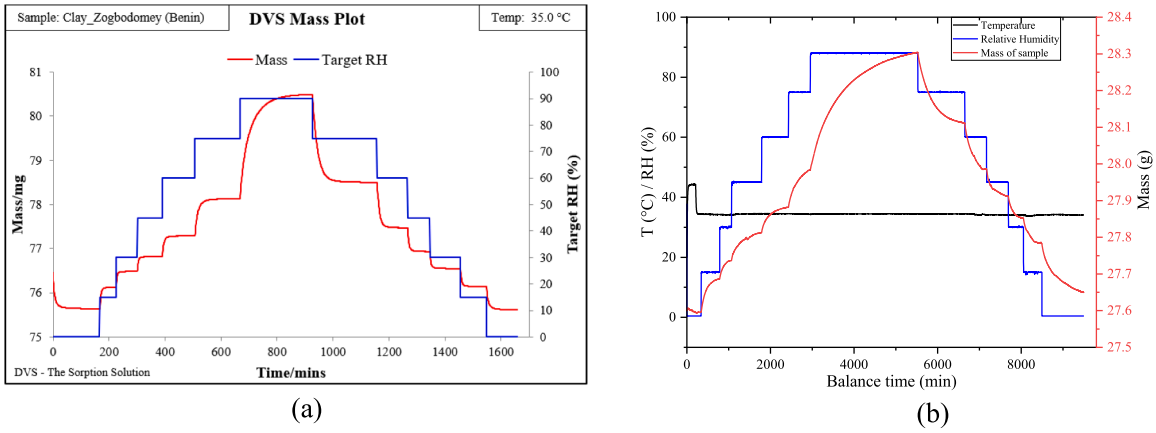

Figure A.1. Changes in moisture and mass (a) in the DVS intrinsic for Clay; (b) in V-GA2 for $CEB_8 - 1$

Data availability

Data will be made available on request.

References

[1] Global Alliance for Building and Construction, Global Status Report for Buildings and Construction, UN environment programme (2024) doi: 10.59117/20.500.11822/45095.
[2] J. Chai, J. Fan, Advanced thermal regulating materials and systems for energy saving and thermal comfort in buildings, Mater. Today Energy 24 (2022) 100925, https://doi.org/10.1016/j.mtener.2021.100925.
[3] S. Wang, C. Yan, F. Xiao, Quantitative energy performance assessment methods for existing buildings, Energy Build. 55 (2012) 873–888, https://doi.org/10.1016/j.enbuild.2012.08.037.
[4] International Energy Agency, Total Energy Use in Buildings: Analysis and Evaluation Methods (Annex 53) EBC Annex (2016) 53.
[5] R. Horne, C. Hayles, Towards global benchmarking for sustainable homes: An international comparison of the energy performance of housing, J. Hous. Built Environ. 23 (2008) 119–130, https://doi.org/10.1007/s10901-008-9105-1.
[6] A. Shahcheraghian, R. Ahmadi, A. Malekpour, Utilising latent thermal energy storage in building envelopes to minimise thermal loads and enhance comfort, J. Energy Storage 33 (2021) 102119, https://doi.org/10.1016/j.est.2020.102119.
[7] Q. Li, L. Zhang, L. Zhang, X. Wu, Optimizing energy efficiency and thermal comfort in building green retrofit, Energy 237 (2021), https://doi.org/10.1016/j.energy.2021.121509.
[8] G.H. Merabet, M. Essaaidi, M.B. Haddou, B. Qolomany, J. Qadir, M. Anan, A. Al-Fuqaha, M.R. Abid, D. Benhaddou, Intelligent building control systems for thermal comfort and energy-efficiency: A systematic review of artificial intelligence-assisted techniques, Renew. Sustain. Energy Rev. 144 (2021) 110969, https://doi.org/10.1016/j.rser.2021.110969.
[9] H. Niroumand, J.A. Barcelo, C.J. Kibert, M. Saaly, Evaluation of Earth Building Tools in Construction (EBTC) in earth architecture and earth buildings, Renew. Sustain. Energy Rev. 70 (2017) 861–866, https://doi.org/10.1016/j.rser.2016.11.267.
[10] L. Zhang, L. Yang, B.P. Jelle, Y. Wang, A. Gustavsen, Hygrothermal properties of compressed earthen bricks, Constr. Build. Mater. 162 (2018) 576–583, https://doi.org/10.1016/j.conbuildmat.2017.11.163.
[11] F. Collet, L. Serres, J. Miriel, M. Bart, Study of thermal behaviour of clay wall facing south, Build. Environ. 41 (2006) 307–315, https://doi.org/10.1016/j.buildenv.2005.01.024.
[12] A. Laborel-Préneron, C. Magniont, J.E. Aubert, Hygrothermal properties of unfired earth bricks: Effect of barley straw, hemp shiv and corn cob addition, Energy Build. 178 (2018) 265–278, https://doi.org/10.1016/j.enbuild.2018.08.021.
[13] H. Cagnon, J.E. Aubert, M. Coutand, C. Magniont, Hygrothermal properties of earth bricks, Energy Build. 80 (2014) 208–217, https://doi.org/10.1016/j.enbuild.2014.05.024.

[14] S. Liuzzi, M.R. Hall, P. Stefanizzi, S.P. Casey, Hygrothermal behaviour and relative humidity buffering of unfired and hydrated lime-stabilised clay composites in a Mediterranean climate, Build. Environ. 61 (2013) 82–92, https://doi.org/10.1016/j.buildenv.2012.12.006.
[15] D. Medjelekh, L. Ulmet, F. Dubois, Characterization of hygrothermal transfers in the unfired earth, Energy Procedia 139 (2017) 487–492, https://doi.org/10.1016/j.egypro.2017.11.242.
[16] F. El Fgaier, Z. Lafhaj, C. Chapiseau, E. Antczak, Effect of sorption capacity on thermo-mechanical properties of unfired clay bricks, J. Build. Eng. 6 (2016) 86–92, https://doi.org/10.1016/j.jobe.2016.02.011.
[17] B. Jiang, R. Lu, M. Jiang, L. Wang, L. Chun, L. Wan, Experimental study on thermal and humidity properties of modified rammed earth buildings in winter, Build. Environ. 258 (2024) 111583, https://doi.org/10.1016/j.buildenv.2024.111583.
[18] A.E. Losini, A.C. Grillet, L. Vo, G. Dotelli, M. Woloszyn, Biopolymers impact on hygrothermal properties of rammed earth: from material to building scale, Build. Environ. 233 (2023) 110087, https://doi.org/10.1016/j.buildenv.2023.110087.
[19] A. Azil, K. Touati, N. Sebaibi, M. Le Guern, F. Streiff, S. Goodhew, M. Gomina, M. Boutouil, Monitoring of drying kinetics evolution and hygrothermal properties of new earth-based materials using climatic chamber simulation, Case Stud. Constr. Mater. 18 (2023) e01798, https://doi.org/10.1016/j.cscm.2022.e01798.
[20] Y.E. Belarbi, M. Sawadogo, P. Poullain, N. Issaadi, A. Hamami, S. Bonnet, R. Belarbi, Experimental characterization of Raw Earth properties for modeling their hygrothermal behavior, Buildings 12 (2022), https://doi.org/10.3390/buildings12050648.
[21] M. Charai, A. Mezrhab, L. Moga, A structural wall incorporating biosourced earth for summer thermal comfort improvement: Hygrothermal characterization and building simulation using calibrated PMV-PPD model, Build. Environ. 212 (2022) 108842, https://doi.org/10.1016/j.buildenv.2022.108842.
[22] C. Turco, A.C. Paula Junior, E.R. Teixeira, R. Mateus, Optimisation of Compressed Earth Blocks (CEBs) using natural origin materials: A systematic literature review, Constr. Build. Mater. 309 (2021) 125140, https://doi.org/10.1016/j.conbuildmat.2021.125140.
[23] A.C. Houngan, M. Anjorin, N. Chitou, Isothermes de sorption de la latérite stabilisée au ciment et du composite ciment bois à l'aide d'une balance à suspension magnétique, SFT (2011) 1–6.
[24] C. Labintan, R. Benelmir, M. Gibigaye, "characterization of the "Banco", A Build. Mater. A Trop. Rural Environ. IJEEE 23 (2015) 203–213, https://hal.univ-lorraine.fr/hal-01595939v1.
[25] C. Toukourou, B.F.Z. FAGLA, G. Bagan, S. Raoul, L. Adjovi, S.J. Avamasse, Mechanical characterization of an eco- material: Case of compress earth bloc (CEB) with addition of cotton waste, Int. J. Cur. Tr. Res. 4 (2015) 109–114.
[26] C. Toukourou, G. Semassou, C. Ahouannou, S. Avamasse, A. Vianou, G. Degan, Thermomechanical characterisation of compressed Earth blocks added with sawdust, Phys. Sci. Int. J. 12 (2016) 1–9, https://doi.org/10.9734/psij/2016/29393.
[27] A.B. Laibi, P. Poullain, N. Leklou, M. Gomina, D.K.C. Sohounhloué, Influence of the kenaf fiber length on the mechanical and thermal properties of Compressed Earth Blocks (CEB), KSCE J. Civ. Eng. 22 (2018) 785–793, https://doi.org/10.1007/s12205-017-1968-9.
[28] G.S.G. Milohin, M. Anjorin, V.S. Gbaguidi, S.C. Adissin, A. Donnot, R. Benelmir, Effect of the addition of glass bottle particles on the mechanical strengths of compressed blocks of fired clay and stabilized earth, Int. J. Adv. Res. 5 (2017) 860–870, https://doi.org/10.21474/IJAR01/5841.
[29] M. Anjorin, C. Akanho, T. Aristide, A.C. Houngan, Characterization of cooked bricks with incorporation of expanded polystyrene for use in buildings, J. Mater. Sci. Surf. Eng. 6 (2018) 743–748.
[30] G.S.G. Milohin, M. Anjorin, V.S. Gbaguidi, A. Donnot, R. Benelmir, Valorisation des cendres issues de la combustion du charbon de bois dans la fabrication de briques d'argile cuite, Rev. Int. Sci. Appl. 1 (2018), 03–10.
[31] P. Poullain, N. Leklou, A.B. Laibi, M. Gomina, Properties of compressed Earth blocks made of traditional materials from benin, Rev. Des. Compos. Et. Des. Mat. ériaux AvancéS. 29 (2019) 233–241, https://doi.org/10.18280/rcma.290407.
[32] C.A. Labintan, C.E. Adadja, M. Gibigaye, H. Zahrouni, M. Hattab, The influence of rice straw on the physical and mechanical properties of Banco, an Adobe reinforced with Rice Straw, Int. J. Eng. Adv. Tech. 9 (2019) 2363–2367, https://doi.org/10.35940/ijeat.A2242.129219.
[33] A. Christian, T.A. Dègodji, T.C. Akanho, Physical and mechanical properties of compacted concrete containing waste glass and laterite as replacements of sand, Int. J. Adv. Mater. Res. 6 (2020) 16–22, https://doi.org/10.35940/ijeat.A2242.129219.
[34] A.A. Djossou, K.V. Doko, D.Y.S. Wade, B. Michozounnou, A. Vianou, Thermal characterization of an eco concrete based on lateritic gravel, millet pods and cement, Am. J. Eng. Appl. Sci. 14 (2021) 398–408, https://doi.org/10.3844/ajeassp.2021.398.408.
[35] G. Kiki, P. Nshimiyimana, C. Kouchadé, A. Messan, A. Houngan, P. André, Physico – mechanical and durability performances of compressed earth blocks incorporating quackgrass straw: An alternative to fired clay, Constr. Build. Mater. 403 (2023) 133064, https://doi.org/10.1016/j.conbuildmat.2023.133064.
[36] B. Chéïssou, K. Tamou, J. Mechling, C.P. Yabi, G. Edjrossè, Use of additive based on non-timber forest products for the ecological stabilization of Raw Earth: Case of the Parkia biglobosa Nut and Vitellaria paradoxa, 4143–4160, J. Renew. Mater. 11 (2023), https://doi.org/10.32604/jrm.2023.030509.
[37] M.K. Kumaran, M.T. Bomberg, Building Envelope and Environmental Control: Part 2 Estimating Performance of Thermal Insulation, Constr. Can. 35 (1993) 24–27.
[38] D. Allinson, M. Hall, Hygrothermal analysis of a stabilised rammed earth test building in the UK, Energy Build. 42 (2010) 845–852, https://doi.org/10.1016/j.enbuild.2009.12.005.
[39] S.I. Kaitouni, M. Charai, N. Es-sakali, M.O. Mghazli, M. El Mankibi, S. Uk-Joo, M. Ahachad, J. Brigui, Energy and hygrothermal performance investigation and enhancement of rammed earth buildings in hot climates: From material to field measurements, Energy Build. 315 (2024) 114325, https://doi.org/10.1016/j.enbuild.2024.114325.
[40] Y.E. Belarbi, M.Y. Ferroukhi, N. Issaadi, P. Poullain, S. Bonnet, Assessment of hygrothermal performance of raw earth envelope at overall building scale, Energy Build. 310 (2024), https://doi.org/10.1016/j.enbuild.2024.114119.
[41] NF XP P13-901, Blocs De. Terre comprimée pour murs Et. cloisons (2001).
[42] P. Nshimiyimana, A. Messan, L. Courard, Physico-mechanical and hygro-thermal properties of compressed earth blocks stabilized with industrial and agro by-product binders, Mater. (Basel) 13 (2020) 1–17, https://doi.org/10.3390/ma13173769.
[43] T. Colinart, M. Pajeot, T. Vinceslas, A. Hellouin De Menibus, T. Lecompte, Thermal conductivity of biobased insulation building materials measured by hot disk: Possibilities and recommendation, J. Build. Eng. 43 (2021) 102858, https://doi.org/10.1016/j.jobe.2021.102858.
[44] B. Rudy, L. Matthieu, A. Jean-Emmanuel, Comparison of the Saturated Salt Solution and the Dynamic Vapor Sorption techniques based on the measured sorption isotherm of barley straw, Constr. Build. Mater. 141 (2017) 140–151, https://doi.org/10.1016/j.conbuildmat.2017.03.005.
[45] M.R. Ahmad, B. Chen, Influence of type of binder and size of plant aggregate on the hygrothermal properties of bio-concrete, Constr. Build. Mater. 251 (2020) 118981, https://doi.org/10.1016/j.conbuildmat.2020.118981.
[46] E. Arthur, M. Tuller, P. Moldrup, L.W. de Jonge, Evaluation of theoretical and empirical water vapor sorption isotherm models for soils, Water Resour. Res. 52 (2016) 190–205, https://doi.org/10.1002/2015WR017681.
[47] Y. Aït Oumeziane, A. Pierre, F. El Mankibi, V. Lepiller, M. Gasnier, P. Désévaux, Hygrothermal properties of an early 20th century clay brick from eastern France: Experimental characterization and numerical modelling, Constr. Build. Mater. 273 (2021) 121763, https://doi.org/10.1016/j.conbuildmat.2020.121763.
[48] M. Charai, A. Mezrhab, L. Moga, A structural wall incorporating biosourced earth for summer thermal comfort improvement: Hygrothermal characterization and building simulation using calibrated PMV-PPD model, Build. Environ. 212 (2022) 108842, https://doi.org/10.1016/j.buildenv.2022.108842.
[49] M. Ben Mansour, A. Jelidi, A.S. Cherif, S. Ben Jabrallah, Optimizing thermal and mechanical performance of compressed earth blocks (CEB), Constr. Build. Mater. 104 (2016) 44–51, https://doi.org/10.1016/j.conbuildmat.2015.12.024.
[50] E. Harb, C. Maalouf, C. Bliard, E. Kinab, M. Lachi, G. Polidori, Hygrothermal performance of multilayer wall assemblies incorporating starch/beet pulp in France, Constr. Build. Mater. 445 (2024) 137773, https://doi.org/10.1016/j.conbuildmat.2024.137773.
[51] EN ISO 12572, (2001). Performance hygrothermique des matériaux et produits pour le bâtiment - Détermination des propriétéS. De. Transm. De. la Vap. D. 'eau 18.
[52] S. Zohoun, E. Agoua, G. Degan, P. Perre, An experimental correction proposed for an accurate determination of mass diffusivity of wood in steady regime, Heat. Mass Transf. 39 (2003) 147–155, https://doi.org/10.1007/s00231-002-0324-9.
[53] H.M. Künzel, A.N. Karagiozis, A. Holm, A Hygrothermal Design Tool for Architects and Engineers, ASTM Int. (2010) 136–151.
[54] E. Malbila, S. Delvoie, D. Toguyeni, S. Attia, L. Courard, An experimental study on the use of fonio straw and shea butter residue for improving the thermophysical and mechanical properties of compressed Earth Blocks, J. Miner. Mater. Charact. Eng. 08 (2020) 107–132, https://doi.org/10.4236/jmmce.2020.83008.
[55] P. Nshimiyimana, C. Hema, O. Zoungrana, A. Messan, L. Courard, Thermophysical and mechanical properties of compressed earth blocks containing fibres: By-product of okra plant and polymer waste, WIT Trans. Built Environ. 195 (2020) 149–161, https://doi.org/10.2495/ARC200121.
[56] B. Taallah, A. Guettala, The mechanical and physical properties of compressed earth block stabilized with lime and filled with untreated and alkali-treated date palm fibers, Constr. Build. Mater. 104 (2016) 52–62, https://doi.org/10.1016/j.conbuildmat.2015.12.007.
[57] T. Ashour, A. Korjenic, S. Korjenic, W. Wu, Thermal conductivity of unfired earth bricks reinforced by agricultural wastes with cement and gypsum, Energy Build. 104 (2015) 139–146, https://doi.org/10.1016/j.enbuild.2015.07.016.
[58] S. Ajouguim, S. Talibi, C. Djelal-Dantec, H. Hajjou, M. Waqif, M. Stefanidou, L. Saadi, Effect of Alfa fibers on the mechanical and thermal properties of compacted earth bricks, Mater. Today Proc. 37 (2019) 4049–4057, https://doi.org/10.1016/j.matpr.2020.07.539.
[59] Nils Frantz, (2024) Influen ce des paramètres de fabrication sur les propriétés multi-physiques des bétons biosourcés Thèse de doctorat de l'Université Paris-Saclay 227.
[60] A.B. Costantini Romero, F.M. Francisca, I. Giomi, Hygrothermal properties of soil–cement construction materials, Constr. Build. Mater. 313 (2021) 1–9, https://doi.org/10.1016/j.conbuildmat.2021.125518.
[61] C.A.S. Hill, A. Norton, G. Newman, The water vapor sorption behavior of natural fibers, J. Appl. Polym. Sci. 112 (2009) 1524–1537, https://doi.org/10.1002/app.29725.
[62] W.A.M. McMinn, T.R.A. Magee, Studies on the effect of temperature on the moisture sorption characteristics of potatoes, J. Food Process Eng. 22 (1999) 113–128, https://doi.org/10.1111/j.1745-4530.1999.tb00475.x.

[63] F. Collet, J. Chamoin, S. Pretot, C. Lanos, Comparison of the hygric behaviour of three hemp concretes, Energy Build. 62 (2013) 294–303, https://doi.org/10.1016/j.enbuild.2013.03.010.
[64] A. Fabbri, F. McGregor, Impact of the determination of the sorption-desorption curves on the prediction of the hemp concrete hygrothermal behaviour, Constr. Build. Mater. 157 (2017) 108–116, https://doi.org/10.1016/j.conbuildmat.2017.09.077.
[65] E.J.D.P. Hansen, M.H. Hansen, Unfired clay bricks - moisture properties and compressive strength, in: Proceedings of the 6th Symposium on Building Physics in the Nordic Countries, (2002) 325–334, Trondheim, Norway.
[66] M. Saidi, A.S. Cherif, B. Zeghmati, E. Sediki, Stabilization effects on the thermal conductivity and sorption behavior of earth bricks, Constr. Build. Mater. 167 (2018) 566–577, https://doi.org/10.1016/j.conbuildmat.2018.02.063.
[67] F. McGregor, A. Heath, E. Fodde, A. Shea, Conditions affecting the moisture buffering measurement performed on compressed earth blocks, Build. Environ. 75 (2014) 11–18, https://doi.org/10.1016/j.buildenv.2014.01.009.
[68] J.F. Daian, Condensation and isothermal water transfer in cement mortar Part I - Pore size distribution, equilibrium water condensation and imbibition, Transp. Porous Media 3 (1988) 563–589, https://doi.org/10.1007/BF00959103.
[69] G. Jraba, N. Salem, J. Neji, Effect of Posidonia oceanica on the hygrothermal characterization of compacted earth blocks, 2024, Constr. Build. Mater. 411 (2024) 134569, https://doi.org/10.1016/j.conbuildmat.2023.134569.
[70] B. Jiang, J. Tan, L. Wan, L. Wang, R. Lu, M. Jiang, Hygrothermal parameters measurement and building performance study of modified rammed earth materials, Energy Build. 299 (2023) 113609, https://doi.org/10.1016/j.enbuild.2023.113609.
[71] P.M. Touré, V. Sambou, M. Faye, A. Thiam, M. Adj, D. Azilinon, Mechanical and hygrothermal properties of compressed stabilized earth bricks (CSEB), J. Build. Eng. 13 (2017) 266–271, https://doi.org/10.1016/j.jobe.2017.08.012.